ECS Transactions, 50 (9) 655-662 (2012)
10.1149/05009.0655ecst ©The Electrochemical Society

Single-Shot Readout of Singlet-Triplet Qubit States in a Si/SiGe Double Quantum Dot

Jon R. Prance[1], Zhan Shi[1], C. B. Simmons[1], D. E. Savage[1], M. G. Lagally[1], L. R. Schreiber[2], L. M. K. Vandersypen[2], Mark Friesen[1], Robert Joynt[1], S. N. Coppersmith[1], and M. A. Eriksson[1]

[1] University of Wisconsin-Madison, Madison, Wisconsin 53706, USA
[2] Kavli Institute of Nanoscience, TU Delft, Lorentzweg 1, 2628 CJ Delft, The Netherlands

The spin singlet and triplet states of a two-electron double quantum dot can be used to form a logical qubit that combines fast manipulation and a spin readout mechanism. We demonstrate single-shot readout of the two-electron states of a Si/SiGe double quantum dot using a quantum-point-contact charge sensor and spin-to-charge conversion. From the statistics of multiple single-shot measurements, we find the lifetimes of the spin states as a function of in-plane magnetic field. The lifetimes of the singlet and T_0 triplet are both ~10ms and insensitive to magnetic field. The T_- triplet lifetime increases with magnetic field, reaching ~3s at 1T.

Introduction

The physical properties of silicon make it a promising host material for solid-state spin qubits. In particular, the high abundance of zero-spin nuclei and a low electron spin-orbit coupling mean that spins in silicon experience few interactions with their environment. Single-spin lifetimes up to several seconds have been seen in silicon, both with electrons in quantum dots and donor-bound electrons (1,2,3,4). One versatile realization of a spin qubit uses two electron spins to form a logical qubit with a basis of the singlet and T_0 triplet states (5,6,7,8). A singlet-triplet qubit can be fully manipulated electrically and possesses a spin readout mechanism due to Pauli spin blockade. In this paper we discuss single-shot initialization and readout of a singlet-triplet qubit and we characterize the lifetimes of its states using repeated single-shot measurements (9).

The Double Quantum Dot Device

We form a double quantum dot by laterally confining electrons in the two-dimensional electron gas (2DEG) of a $Si/Si_{0.7}Ge_{0.3}$ heterostructure at a temperature of ≈100 mK. The 2DEG is situated in a 12nm thick, strained silicon quantum well approximately 75 nm below the surface of the heterostructure. Modulation doping with phosphorus approximately 40 nm below the surface populates the electron gas. The lateral confinement of the quantum dots is provided by nano-scale, palladium surface gates operating in depletion mode. The gates are fabricated using an electron-beam lithography lift-off process. Figure 1(a) shows an SEM image of the surface gates on a completed device, similar to the one measured in this experiment.

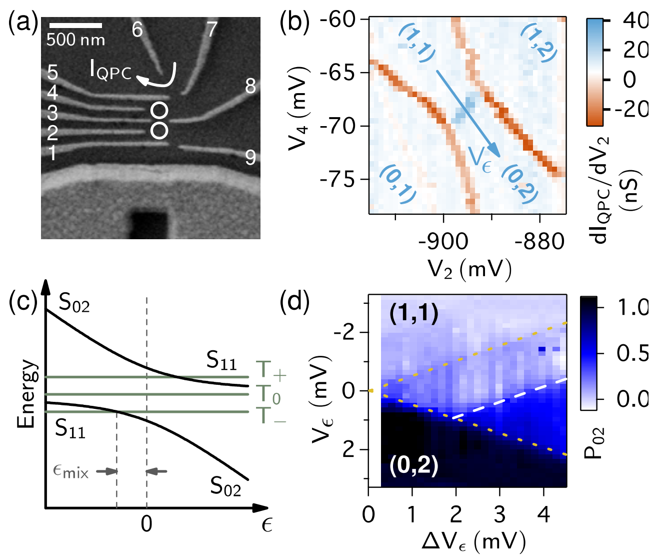

Figure 1. (a) An SEM image of a device similar to the one measured. The palladium gates labeled 1-9 define the double-dot confinement potential and a nearby point-contact charge sensor. The circles indicate the approximate locations of the two quantum dots. The point-contact is formed between gates 5 and 6. The large gate at the bottom of the image is unused. (b) Differentiated charge sensor current I_{QPC} as a function of the voltages on gates 2 and 4. Charge transitions in the double-dot produce signals in the derivative of I_{QPC}. The charge occupations of each region are labeled (n,m) (n electrons in the upper dot, m electrons in the lower dot). (c) Predicted energies of the double-dot states as a function of detuning energy ε in a non-zero magnetic field. The detuning energy is varied by moving along the direction $V\varepsilon$ shown in (b). $\varepsilon=0$ is at the (1,1)-(0,2) transition. (d) Time-averaged probability of finding the system in the (0,2) charge state while applying square pulses of detuning with amplitude $\Delta V\varepsilon$. Inter-dot tunneling occurs inside the dotted triangle, which should give $P_{02}=0.5$ for symmetric tunneling. The suppression of P_{02} above the dashed line is due to Pauli spin blockade of (1,1) to (0,2) transitions. The separation between the dashed line and the upper edge of the triangle is the (0,2) singlet-triplet splitting energy E_{ST}, which we find to be 124±4 μeV. Reprinted with permission from Ref. (9). Copyright (2012) by the American Physical Society.

The surface gates can be used to form a quantum-point-contact (QPC) charge sensor near the double dot. The conduction of the QPC is very sensitive to changes in local electric potential, and we use it to detect changes in charge occupation of the quantum dots. Figure 1(b) shows the differentiated QPC current as a function of two gate voltages, each of which has the primary effect of changing the energy of one of the dots. In this experiment we focus on the crossover between a charge occupation of (1,1) (one electron on each dot) and (0,2) (both electrons on one of the dots). The dot occupations are found by counting transitions to the (0,0) region.

Single-Shot Measurement and Initialization of Qubit States

To measure the spin of the qubit states we use the QPC charge sensor and spin-to-charge conversion enabled by Pauli spin blockade (10,11,12). Figure 1(c) shows the expected energies of the two-electron double-dot states near the crossover between (1,1) and (0,2) charge occupations (13). The energies are shown as a function of detuning energy ε, which corresponds to the direction marked $V\varepsilon$ in Figure 1(b). Near the (1,1)-(0,2) crossover (at ε=0) the accessible states are a spin singlet in the (1,1) charge configuration (S_{11}), three (1,1) spin triplets (T_-, T_0 and T_+), and a (0,2) spin singlet (S_{02}). The (0,2) triplet states are not accessible because they include an additional orbital excitation that raises their energy significantly. S_{11} and S_{02} anti-cross due to inter-dot tunnel coupling. Starting in the (1,1) charge configuration, we read the spin state by pulsing V_2 and V_4 to positive detuning where the ground state is S_{02}. The system will only be able to tunnel from (1,1) to (0,2) if it starts in a singlet S_{11}, because spin must be conserved. If the initial state is one of the three (1,1) triplets, then the system will remain in (1,1) for the lifetime of the triplet state. By measuring the charge sensor in real time, we can detect whether this spin blockade occurred and infer the spin of the initial (1,1) state.

The system can be initialized to S_{11} by reversing the above process: starting in the (0,2) charge configuration the system is allowed to relax to the ground state S_{02}. This singlet is then transferred to S_{11} by pulsing V_2 and V_4 into the (1,1) region ($\varepsilon<0$).

Figures 2(a) and 2(b) show typical results of performing single-shot initialization and readout as described above. Both plots show the QPC current as a function of time as V_2 and V_4 are pulsed across the (1,1)-(0,2) transition. The pulse sequence first initializes the system to S_{11} at a time ≈1 ms. The spin state is then read out ≈1.7 ms later. In Figure 2(b) the system quickly tunnels to (0,2) during the readout phase, suggesting that the (1,1) spin state was S_{11}. In Figure 2(a) the system remains blockaded in (1,1) during the readout, suggesting that the (1,1) spin state is a triplet. This means that the spin of the system changed since it was initialized.

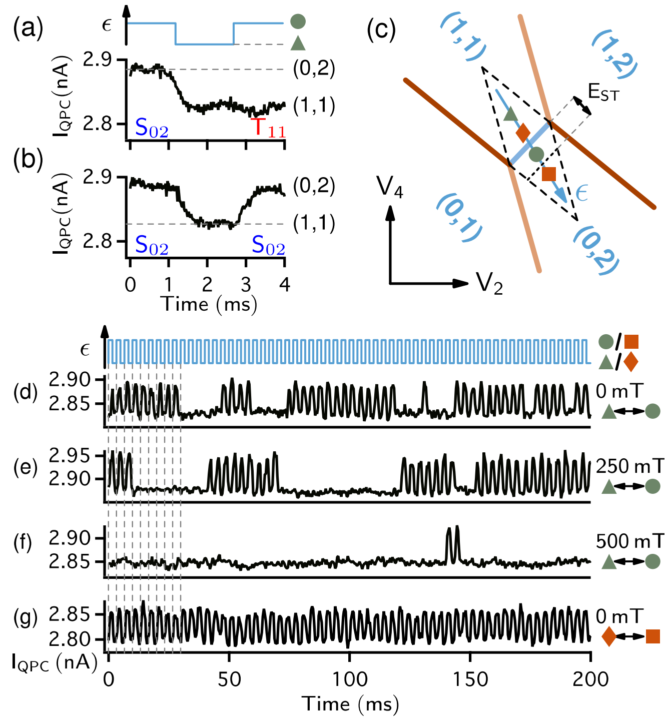

Figure 2. (a) and (b) Charge sensor current I_{QPC} as the system is pulsed between positive and negative detuning ε. Low current indicates a (1,1) charge state and high current indicates (0,2). In (a) the electron does not tunnel back to the (0,2) charge state because of spin blockade that occurs when the spin state of the two electrons is a triplet. The two detuning values of the pulse cycle are indicated on the schematic stability diagram (c) by the circular and triangular points. Charge transitions occur primarily by inter-dot tunneling within the dashed triangles in (c). We keep the two detuning values inside this region. (d)-(f) Charge sensor signals over multiple pulse cycles with different in-plane magnetic fields. Data at all fields show extended periods of blockade due to long-lived spin triplet states (low current) and free charge tunneling of spin singlet states. With increasing field, the durations of the blockaded periods increase significantly. (g) As a consistency check, the detuning pulse was shifted to more positive ε until the (0,2) triplets were available for tunneling. In this situation, charge transitions may occur regardless of the spin state and we observe no spin blockade. The shift in detuning is determined by the (0,2) singlet-triplet splitting energy E_{ST}. Reprinted with permission from Ref. (9). Copyright (2012) by the American Physical Society.

Spin State Lifetimes

We use repeated single-shot spin readout to measure the lifetime of the two-electron spin states. Figure 2(d) shows the charge sensor current I_{QPC} while V_2 and V_4 are pulsed to alternate between positive detuning (ε>0) and negative detuning (ε<0) at a frequency of 300Hz. During the ε<0 half of each pulse cycle, the charge state is always (1,1) and I_{QPC} is always low. During the ε>0 half of each pulse cycle, the spin state is measured: high current indicates a (0,2) singlet, low current indicates a spin-blockaded (1,1) triplet. Figure 2(d) shows extended periods where the system freely switches between (1,1) and

(0,2), and other periods where the system remains blockaded in (1,1) over multiple pulse cycles.

To quantify the lifetimes of the spin states we examine the durations of blockaded and un-blockaded periods in several minutes of charge sensor data. Figure 3(a) and 3(b) show the distributions of durations in 6.4 minutes of real-time charge sensor data at zero magnetic field. Figure 3(a) shows the durations t_b of blockaded periods while 3(b) shows the durations t_u of un-blockaded periods. Both distributions decay exponentially, and from the fitted decay constants we find a typical duration of τ_b = 9.6ms for the blockade periods and τ_u = 23ms for un-blockaded periods. These times can be related to the lifetimes of the S_{11} and (1,1) triplet states by modeling the time evolution of the system during a single pulse cycle. Using a rate-equation model, we find that the S_{11} and (1,1) triplet states mix with each other on a time scale of 25 ms during the $\varepsilon<0$ half of each pulse cycle, and on a time scale of 6 ms during the $\varepsilon>0$ half of each pulse cycle (see reference 9 for details).

These lifetimes are 2 orders of magnitude longer than comparable results seen in GaAs quantum dots. In GaAs, mixing between the singlet and triplet states is caused by the contact hyperfine interaction with background nuclear spins (14,15,16,17,18). The effect is much weaker in silicon because of the high abundance of zero-spin nuclei. Based on predictions and measurements of the hyperfine coupling in silicon quantum dots (~3 neV), we expect that it will be exceeded by the energy difference between the S_{11} state and the (1,1) triplet states over the whole range of detuning in our measurements (8,19). This means that the hyperfine mixing process will be strongly suppressed, leading to the long lifetimes that we observe.

As shown in Figure 2(d-f), the behavior of the system changes significantly with increasing magnetic field. When we repeat the above analysis with data taken at non-zero magnetic field, we find that the distribution of blockaded period durations shows two characteristic time scales. Figure 3(c,d) show the distributions at a magnetic field of 250mT. The first time scale in Figure 3(c) is similar to the zero-field result (τ_b'~10ms), while the second time scale τ_b is longer. Figure 3(e) shows the fitted decay constants as a function of in-plane magnetic field up to 1T. While τ_b' and τ_u are insensitive to the field, τ_b increases significantly reaching several seconds at 1T.

Two time scales arise in the durations of blockade because, at non-zero field, there are two distinct triplet states that lead to spin blockade: the (1,1) T_- and T_0. The energy of the T_- state decreases with increasing field. This decreases the rate at which it can scatter to S_{11} or T_0, increasing its lifetime (10). The T_0 does not change energy with magnetic field and its lifetime is not affected significantly. (The T_+ state does not play a role because it is raised in energy and will be rarely populated.) We interpret the time scale τ_b' as being due to blockade of the T_0 state, and τ_b as being due to blockade of the T_- state. Using a similar rate equation to the one used for the zero-field data, we extract the lifetimes of these states from the fitted values of τ_u, τ_b, and τ_b'. The results show that mixing between the nearly degenerate S_{11} and T_0 states occurs on a time scale of ~10 ms and is not sensitive to the magnetic field. The T_- state lifetime increases with field, reaching ~3 seconds at 1T. This T_- lifetime agrees with single-spin lifetimes measured in silicon nano-devices at similar magnetic fields (1,2,3,4).

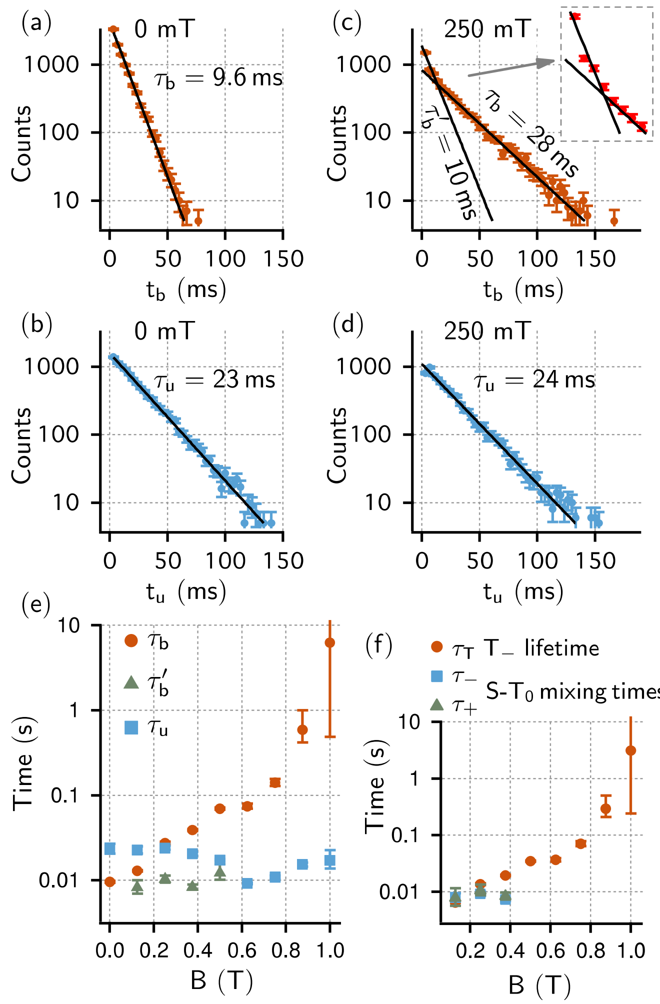

Figure 3. (a,b) Statistics of the durations t_b of blockaded periods and the durations t_u of un-blockaded periods in 6.4 minutes of real-time charge sensor data measured at zero magnetic field. (c,d) Statistics for data measured in a 250mT in-plane magnetic field. The durations of blockaded periods t_b show two distinct time scales due to the Zeeman splitting of the triplet states. (e) Fitted decay constants as a function of magnetic field. At fields above 0.4T it becomes impractical to determine the shorter blockade timescale τ_b' (characterizing T_0 occupation) because the system spends so much time in the long-lived T_- state, characterized by τ_b. (f) Two-electron spin state lifetimes extracted from the data in (e) using a rate-equation model of the time evolution of the system during a single pulse cycle. The S-T_0 mixing time τ_+ (τ_-) characterizes mixing during the $\varepsilon>0$ ($\varepsilon<0$) half of each pulse cycle. Reprinted with permission from Ref. (9). Copyright (2012) by the American Physical Society.

Conclusions

We have argued that the lifetimes of two-electron singlet and T_0 spin states in a silicon double quantum dot at zero magnetic field can be as high as ~10 ms. This long time allows us to perform real-time, single-shot readout of the spin states. The lifetimes of the S_{11} singlet and T_0 triplet states are insensitive to magnetic field, remaining ~10ms up to 0.4T. The T_- triplet becomes increasingly long-lived in increasing magnetic field, reaching a lifetime of ~3s at 1T. The T. lifetime is comparable to single-spin lifetimes measured in silicon at similar fields. The S_{11} and T_0 lifetimes are consistent with mixing of spin states due to hyperfine coupling to background nuclear spins.

Acknowledgments

This work was supported in part by ARO (W911NF-08-1-0482) and by the United States Department of Defense. The views and conclusions contained in this document are those of the authors and should not be interpreted as representing the official policies, either expressly or implied, of the Department of Defense. This research utilized NSF-supported shared facilities at the University of Wisconsin-Madison. L. V. acknowledges financial support by a Starting Grant of the European Research Council (ERC) and by the Foundation for Fundamental Research on Matter (FOM).

References

1. M. Xiao, M. G. House, and H. W. Jiang, *Phys. Rev. Lett.*. **104**, 096801 (2010).
2. A. Morello et al., *Nature (London)* **467**, 687 (2010).
3. C. B. Simmons, J. R. Prance, B. J. Van Bael, T. S. Koh, Z. Shi, D. E. Savage, M. G. Lagally, R. Joynt, M. Friesen, S.N. Coppersmith, and M.A. Eriksson, *Phys. Rev. Lett.*, **106**, 156804 (2011).
4. R. R. Hayes *et al.,* arXiv:0908.0173.
5. J. Levy, *Phys. Rev. Lett.*, **89**, 147902 (2002).
6. J. R. Petta, A. C. Johnson, J. M. Taylor, E. A. Laird, A. Yacoby, M. D. Lukin, C. M. Marcus, M. P. Hanson, and A. C. Gossard, *Science*, **309**, 2180 (2005).
7. S. Foletti, H. Bluhm, D. Mahalu, V. Umansky, and A. Yacoby, *Nature Phys.*, **5**, 903 (2009).
8. B. M. Maune et al., *Nature*, **481**, 344–347 (2012).
9. J. R. Prance, Zhan Shi, C. B. Simmons, D. E. Savage, M. G. Lagally, L. R. Schreiber, L. M. K. Vandersypen, Mark Friesen, Robert Joynt, S. N. Coppersmith, and M. A. Eriksson, *Phys. Rev. Lett.*, **108**, 046808 (2012).
10. N. Shaji et al., *Nature Phys.,* **4**, 540 (2008).
11. M. G. Borselli *et al.*, *Appl. Phys. Lett.,* **99**, 063109 (2011).
12. N. S. Lai, W. H. Lim, C. H. Yang, F. A. Zwanenburg, W. A. Coish, F. Qassemi, A. Morello, and A.S. Dzurak, *Scientific Reports*, **1**, 110 (2011).
13. R. Hanson, L. P. Kouwenhoven, J. R. Petta, S. Tarucha, and L. M. K. Vandersypen, *Rev. Mod. Phys.,* **79**, 1217 (2007).
14. A. C. Johnson, J. R. Petta, J. M. Taylor, A. Yacoby, M. D. Lukin, C. M. Marcus, M. P. Hanson, and A. C. Gossard, *Nature (London),* **435**, 925 (2005).
15. J. R. Petta, A. C. Johnson, A. Yacoby, C. M. Marcus, M. P. Hanson, and A.C. Gossard, *Phys. Rev. B*, **72**, 161301 (2005).
16. F. H. L. Koppens, J. A. Folk, J. M. Elzerman, R. Hanson, L.H. Willems van Beveren, I.T. Vink, H.P. Tranitz, W. Wegscheider, L. P. Kouwenhoven, and L. M. K. Vandersypen, *Science,* **309**, 1346 (2005).
17. W. A. Coish and D. Loss, *Phys. Rev. B,* **72**, 125337 (2005).
18. J. M. Taylor, J. R. Petta, A. C. Johnson, A. Yacoby, C. M. Marcus, and M. D. Lukin, *Phys. Rev. B,* **76**, 035315 (2007).

19. L. V. C. Assali, H. M. Petrilli, R. B. Capaz, B. Koiller, X. Hu, and S. Das Sarma, *Phys. Rev. B,* **83**, 165301 (2011).